



Contents lists available at ScienceDirect

Physics Letters A

www.elsevier.com/locate/pla



Spin-orbit-coupled BEC in a double-well potential: Quantum energy spectrum and flat band

Wen-Yuan Wang^{a,b}, Hui Cao^b, Jie Liu^{a,b,c}, Li-Bin Fu^{b,c}

^a School of Physics, Beijing Institute of Technology, Beijing 100081, China

^b National Laboratory of Science and Technology on Computational Physics, Institute of Applied Physics and Computational Mathematics, Beijing 100088, China

^c Center for Applied Physics and Technology, Peking University, Beijing 100084, China

ARTICLE INFO

Article history:

Received 25 March 2015

Accepted 18 April 2015

Available online xxxx

Communicated by R. Wu

Keywords:

Energy spectrum

Flat band

Spin-orbit-coupled BEC

Double-well potential

ABSTRACT

Spin-orbit-coupled Bose-Einstein condensates (BECs) provide a powerful platform for studies on physical problems in various fields. Here we study the energy spectrum of a tunable spin-orbit-coupled BEC in a double-well potential with adjustable Raman laser intensity. We find in the single-particle spectrum there is a highly degenerate flat band in the ground state of the BEC, which remains stable against changes of the Raman strength. Many-body interactions between atoms remove this high degeneracy. Analytical results for particular cases are obtained by using the perturbation theory, which are in good agreement with the numerical results.

© 2015 Elsevier B.V. All rights reserved.

1. Introduction

Benefited from the development of artificial gauge fields [1–7], experiments have successfully realized an ⁸⁷Rb Bose-Einstein condensate (BEC) with spin-orbit coupling [8]. The same scheme has been subsequently extended to realize spin-orbit-coupled (SOC) Fermi gases [9,10]. These experimental achievements have stimulated a growing interest in researches on spin-orbit-coupled quantum gases, such as quantum phase transition [11], topological excitations [12], Majorana fermions [13], and spintronic devices [14].

Recently, SOC BECs in a double-well potential have been investigated [15–19], focusing on the quantum dynamics, Josephson effects, and macroscopic self-trapping with weak and strong Raman strength. SOC BECs in a double-well potential provide insight into the phenomena of the interplay between interatomic interactions and spin-orbit coupling, and thus serve as a platform for quantum simulation and are worth more in-depth investigation.

In this Letter, we study a tunable SOC BEC in a double-well potential through modulation of the Raman laser intensity, which can be easily implemented in experiments [8]. Here we focus on the energy spectrum of an SOC BEC in a double-well potential, which may provide an insight into the dynamics. For the linear case, with the changes of the Raman strength, there is a flat band for the ground state of the BEC. In this case, a system of N non-interacting bosons is characterized by an $(N + 1)$ -fold degenerate

state. Weak interactions between atoms remove this large degeneracy. However, for a group of energy levels that lie on the same flat band in the linear case, energy difference is very small. With the help of perturbation theory, some analytical results are obtained, which agree well with the numerical results.

The outline of the Letter is as follows. First, we introduce the total Hamiltonian for an N -atom SOC BEC in a symmetrical double-well potential. Following this, we numerically diagonalize the Hamiltonian and study the energy spectrum of the SOC BEC without interactions, and flat band is analyzed in-depth. Then, we study the lowest flat band in the presence of atom interactions. Some analytical results are obtained with the help of perturbation theory. Finally, we give a brief conclusion.

2. The total Hamiltonian

Spin-orbit coupling in the ultracold ⁸⁷Rb atoms was experimentally realized recently at NIST [2], in which the Raman dressing scheme is based on coupling two atomic hyperfine states of $5S_{1/2}$, $|F = 1, m_F = 0\rangle$ and $|F = 1, m_F = -1\rangle$, labeled as spin-up $|\uparrow\rangle$ and spin-down $|\downarrow\rangle$, respectively. We consider such an SOC BEC in a double-well potential, with the wells indicated by l and r , respectively. To investigate the dynamics of the system, we adopt the two-mode approximation. Then, the total Hamiltonian for such an N -atom SOC BEC in a symmetrical double-well potential can be written as

$$\hat{H} = \hat{H}_0 + \hat{H}_{\text{int}}. \quad (1)$$

E-mail addresses: hcao.physics@gmail.com (H. Cao), lbfu@iapcm.ac.cn (L.-B. Fu).

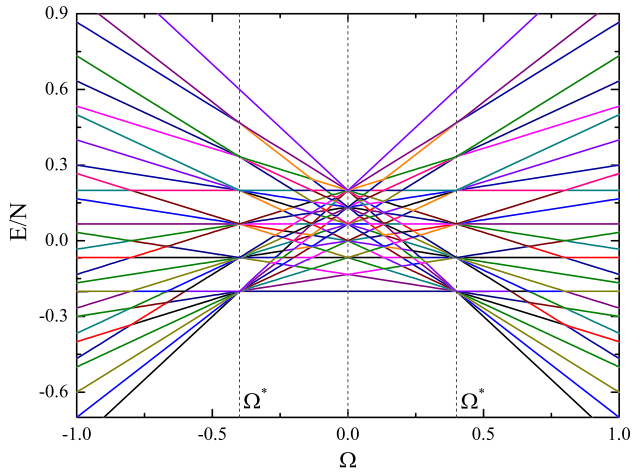


Fig. 1. (Color online.) Energy spectrum in the non-interaction case, where $J = 0.2$, $\beta = 0.5$, and $N = 6$.

The single-atom Hamiltonian is given by

$$\begin{aligned} \hat{H}_0 = & J_{\uparrow\uparrow}(\hat{a}_{l\uparrow}^\dagger \hat{a}_{r\uparrow} + \hat{a}_{l\uparrow} \hat{a}_{r\uparrow}^\dagger) + J_{\downarrow\downarrow}(\hat{a}_{l\downarrow}^\dagger \hat{a}_{r\downarrow} + \hat{a}_{l\downarrow} \hat{a}_{r\downarrow}^\dagger) \\ & + J_{\uparrow\downarrow}(\hat{a}_{l\uparrow}^\dagger \hat{a}_{r\downarrow} + \hat{a}_{l\uparrow} \hat{a}_{r\downarrow}^\dagger) + J_{\downarrow\uparrow}(\hat{a}_{l\downarrow}^\dagger \hat{a}_{r\uparrow} + \hat{a}_{l\downarrow} \hat{a}_{r\uparrow}^\dagger) \\ & + \frac{\Omega}{2}(\hat{a}_{l\uparrow}^\dagger \hat{a}_{l\downarrow} + \hat{a}_{l\uparrow} \hat{a}_{l\downarrow}^\dagger + \hat{a}_{r\uparrow}^\dagger \hat{a}_{r\downarrow} + \hat{a}_{r\uparrow} \hat{a}_{r\downarrow}^\dagger). \end{aligned} \quad (2)$$

Here the operator $\hat{a}_{j\sigma}$ ($\hat{a}_{j\sigma}^\dagger$) is the annihilation (creation) operator for spin σ ($\sigma = \uparrow, \downarrow$) in the j ($j = l, r$) well, Ω is the Raman coupling strength, $J_{\uparrow\downarrow}$ induced by the Raman coupling is the interwell spin-flip tunneling amplitude, and $J_{\sigma\sigma}$ is the Josephson tunneling amplitude between left and right wells.

The two-body interactions between atoms are described by

$$\begin{aligned} \hat{H}_{\text{int}} = & \frac{1}{2} \sum_j \left(\frac{g_{\uparrow\uparrow}}{N} \hat{a}_{j\uparrow}^\dagger \hat{a}_{j\uparrow}^\dagger \hat{a}_{j\uparrow} \hat{a}_{j\uparrow} + \frac{g_{\downarrow\downarrow}}{N} \hat{a}_{j\downarrow}^\dagger \hat{a}_{j\downarrow}^\dagger \hat{a}_{j\downarrow} \hat{a}_{j\downarrow} \right. \\ & \left. + \frac{2g_{\uparrow\downarrow}}{N} \hat{a}_{j\uparrow}^\dagger \hat{a}_{j\downarrow}^\dagger \hat{a}_{j\uparrow} \hat{a}_{j\downarrow} \right), \end{aligned} \quad (3)$$

where $g_{\sigma\sigma'}$ with $\sigma, \sigma' = \uparrow, \downarrow$ is the interaction strength. For ^{87}Rb atoms, the differences between the spin-dependent nonlinear coefficients are very small and contribute only small modifications to the collective behavior [20]. In the present Letter, we take $g_{\sigma\sigma} = g_{\sigma\sigma'}$.

The above parameters are all tunable in experiments [8], which can be achieved by adjusting the trapping potential and the angle between Raman lasers. The interwell spin-flip tunneling amplitude is linearly dependent on the Raman coupling [15], and we denote it as $J_{\uparrow\downarrow} = \beta\Omega$. For simplicity, we take $J_{\uparrow\uparrow} = J_{\downarrow\downarrow} = J$.

3. Energy spectrum of the SOC BEC

In order to study the energy spectrum of the SOC BEC, one can numerically diagonalize the Hamiltonian in $N_D = (N + 3)(N + 2)(N + 1)/6$ dimensional space spanned by the many-body Fock basis $\{|N_{l\uparrow}, N_{l\downarrow}, N_{r\uparrow}, N_{r\downarrow}\rangle\}$, where $N_{j\sigma}$ is the number of bosons with spin σ in the j well. The eigenfunctions and eigenenergies can be derived as

$$|\psi\rangle = \sum_{k=1}^{N_D} c_k |N_{l\uparrow}, N_{l\downarrow}, N_{r\uparrow}, N_{r\downarrow}\rangle, \quad E = \langle\psi|\hat{H}|\psi\rangle. \quad (4)$$

Without the interactions between atoms, we numerically diagonalize the Hamiltonian \hat{H}_0 . The energy spectrum is shown in Fig. 1 with $J = 0.2$ and $N = 6$ as an example. One can see there are three

groups of degenerate points, at $\Omega = -2J, 0$ and $2J$, respectively. Detailed analysis of these degenerate points is presented in the following of this section. There are a group of flat bands between two critical values of Raman strength $\Omega^* = \pm 2J$. When increasing the absolute value of Raman strength $|\Omega|$, the energy decreases when $|\Omega| > \Omega^*$, while the energy remains stable in the flat band.

The energy spectrum without interactions can be obtained analytically. To this end, we introduce the quasi-particle Bose operators, $\hat{A}_1 = (\hat{a}_{l\uparrow} - \hat{a}_{l\downarrow} + \hat{a}_{r\uparrow} - \hat{a}_{r\downarrow})/2$, $\hat{A}_2 = (-\hat{a}_{l\uparrow} - \hat{a}_{l\downarrow} + \hat{a}_{r\uparrow} + \hat{a}_{r\downarrow})/2$, $\hat{A}_3 = (\hat{a}_{l\uparrow} - \hat{a}_{l\downarrow} - \hat{a}_{r\uparrow} + \hat{a}_{r\downarrow})/2$, and $\hat{A}_4 = (\hat{a}_{l\uparrow} + \hat{a}_{l\downarrow} + \hat{a}_{r\uparrow} + \hat{a}_{r\downarrow})/2$. These operators obey the usual commutation relation $[\hat{A}_i, \hat{A}_j^\dagger] = \delta_{ij}$. By using these operators, the above Hamiltonian (2) is rewritten in a more convenient form as

$$\begin{aligned} \hat{H}_0^A = & (J - \beta\Omega - \frac{\Omega}{2})\hat{n}_1 + (-J - \beta\Omega + \frac{\Omega}{2})\hat{n}_2 \\ & + (-J + \beta\Omega - \frac{\Omega}{2})\hat{n}_3 + (J + \beta\Omega + \frac{\Omega}{2})\hat{n}_4. \end{aligned} \quad (5)$$

Here, $\hat{n}_i \equiv \hat{A}_i^\dagger \hat{A}_i$ is the quasi-particle number operator. From Eq. (5), the Hamiltonian without interaction is strictly diagonalized. For the cases we study in the present Letter, i.e. $\beta = 0.5$, the Hamiltonian (5) can be simplified to the following form

$$\hat{H}_0^A = J(\hat{n}_1 - \hat{n}_2 - \hat{n}_3 + \hat{n}_4) - \Omega(\hat{n}_1 - \hat{n}_4). \quad (6)$$

For the groups of degenerate points at critical values $\Omega = \pm 2J$, energy $E = -J(N - 4\hat{n}_4)$ can be obtained from Eq. (6) along with the particle number conserved condition. As the value of \hat{n}_4 is in the range from 0 to N , there are $N + 1$ points at the critical Raman strength $\Omega = 2J$. The i -th point has $[(N + 2 - i)(N + 1 - i)/2]$ -fold degeneracy, here $i = 0, 1, 2, \dots, N$ for energy from low to high. For the group of degenerate points at the critical Raman strength $\Omega = 0$, one also obtain the energy $E = -J[N - 2(\hat{n}_1 + \hat{n}_4)]$ from Eq. (6) together with the particle-number conservation condition. As the value of $\hat{n}_1 + \hat{n}_4$ is in the range from 0 to N , there are also $N + 1$ points and the i -th point has $[(i + 1)(N - i + 1)]$ -fold degeneracy.

As for the flat bands, since the energy is independent on the Raman strength, the condition $\hat{n}_1 = \hat{n}_4$ is required in Eq. (6). For each flat band, the energy can be obtained: $E = -J(N - 4\hat{n}_4)$. The number of flat bands is related to the parity of the particle number, i.e. $(N + 1)/2$ or $N/2 + 1$ for the quasi-particle number being odd or even. For the i -th flat band, the value of energy is $-J(N - 4i)$ with $(N - 2i + 1)$ -fold degeneracy (here $i = 0, 1, 2, \dots, N$ for energy from low to high). In the following, we mainly focus on the lowest flat band. The condition $\hat{n}_1 = \hat{n}_4 = 0$ is satisfied. The lowest flat band energy is $-JN$ with $(N + 1)$ -fold degeneracy.

4. Flat band with the interaction between atoms

When the atomic interaction is included, the degeneracy of the flat band will be removed. In Fig. 2, we show the energy spectrum for an SOC BEC with $g = 0.05$, $J = 0.2$, and $N = 6$ as an example.

It is clear that the interactions remove the degeneracy of the flat band, and shift the spectrum upwards as well. However, for a group of energy levels that lie on the same flat band in the linear case, energy difference between separated energy levels is actually quite small. In Fig. 3, we show the difference between the energy maximum E_{N+1} and minimum E_1 of the lowest band $\Delta = E_{N+1} - E_1$.

In the region $|\Omega| > \Omega^*$, the difference Δ is larger than that in the flat-band region $|\Omega| < \Omega^*$. With changes of Raman strength, the difference changes relatively slow in the flat band, while it changes fast in the other regime. We also notice the difference decreases with the increasing of the particle number.

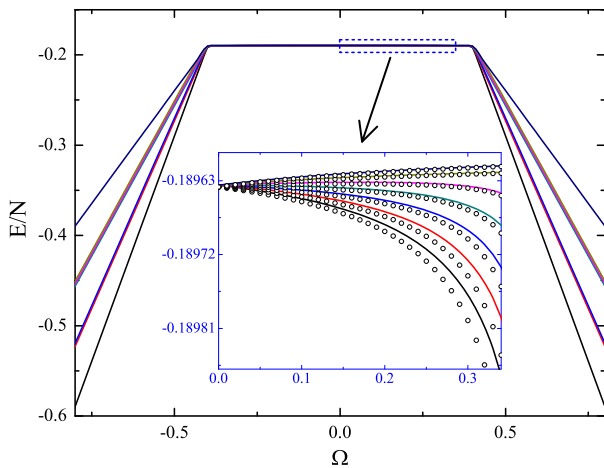


Fig. 2. (Color online.) Lowest flat-band energy spectrum with atom interaction, where $J = 0.2$, $\beta = 0.5$, $g = 0.05$, and $N = 6$.

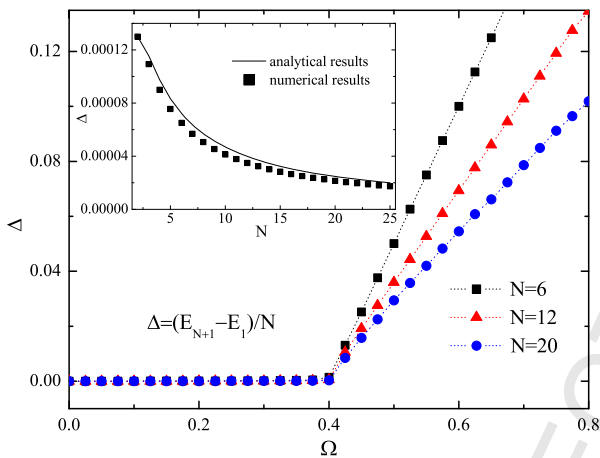


Fig. 3. (Color online.) Energy difference between the energy maximum E_{N+1} and minimum E_1 of the lowest band $\Delta = E_{N+1} - E_1$, where $J = 0.2$, $\beta = 0.5$, and $g = 0.05$. The inset shows energy difference of lowest flat-band versus particle number N when Raman strength $\Omega = 0.5\Omega^*$.

For quite weak interaction, perturbation theory is applicable with the atomic interaction as the perturbation terms. In the quasi-particle representation, the two-body interaction Hamiltonian becomes

$$\begin{aligned} \hat{H}_{\text{int}}^A = & \frac{g}{4N} \left(\sum_i \hat{A}_i^\dagger \hat{A}_i^\dagger \hat{A}_i \hat{A}_i + \hat{A}_1^\dagger \hat{A}_1^\dagger \hat{A}_3 \hat{A}_3 + \hat{A}_3^\dagger \hat{A}_3^\dagger \hat{A}_1 \hat{A}_1 \right. \\ & + \hat{A}_2^\dagger \hat{A}_2^\dagger \hat{A}_4 \hat{A}_4 + \hat{A}_4^\dagger \hat{A}_4^\dagger \hat{A}_2 \hat{A}_2 + 2\hat{n}_1 \hat{n}_2 + 4\hat{n}_1 \hat{n}_3 \\ & + 2\hat{n}_1 \hat{n}_4 + 2\hat{n}_2 \hat{n}_3 + 4\hat{n}_2 \hat{n}_4 + 2\hat{n}_3 \hat{n}_4 + 2\hat{A}_1^\dagger \hat{A}_2^\dagger \hat{A}_3 \hat{A}_4 \\ & \left. + 2\hat{A}_1^\dagger \hat{A}_4^\dagger \hat{A}_2 \hat{A}_3 + 2\hat{A}_2^\dagger \hat{A}_3^\dagger \hat{A}_1 \hat{A}_4 + 2\hat{A}_3^\dagger \hat{A}_4^\dagger \hat{A}_1 \hat{A}_2 \right). \end{aligned}$$

As previously discussed, for the lowest flat band, no particles distribute in the quasi-particle modes A_1 and A_4 , and the degenerate subspace for the lowest flat band is constructed by $|j\rangle = |0, j, N-j, 0\rangle$, i.e.,

$$|j\rangle = \frac{1}{\sqrt{j!(N-j)!}} (\hat{A}_2^\dagger)^j (\hat{A}_3^\dagger)^{N-j} |\text{vac}\rangle. \quad (7)$$

In the spirit of the degenerate perturbation theory, the first-order perturbation can be obtained by letting degenerate subspace $\{|j\rangle\}$ be the complete collection of degenerate eigenstates of \hat{H}_{int}^A . The required energy correction in first-order approximation is given by

$$E_j^{(1)} = \langle j | \hat{H}_{\text{int}}^A | j \rangle = \frac{g}{4} (N-1).$$

We notice that the first-order perturbation does not remove the high degeneracy of the flat band. In this case, we naturally take into consideration the influence of the states $\{|k\rangle\}$ which do not belong to the flat band $\{|j\rangle\}$. Then, the required energy correction is given by

$$\begin{aligned} E_j^{(2)} &= \sum_{j \neq k} \frac{\langle j | \hat{H}_{\text{int}}^A | k \rangle \langle k | \hat{H}_{\text{int}}^A | j \rangle}{E_j^{(0)} - E_k^{(0)}} \\ &= \left(\frac{g}{4N} \right)^2 \left(\frac{(N-j)(N-j-1)}{\Omega - 2J} - \frac{j(j-1)}{\Omega + 2J} - \frac{j(N-j)}{J} \right). \end{aligned}$$

Now the degeneracy of flat band is totally removed. The perturbed energy in the flat band is

$$E_j = E_j^{(0)} + E_j^{(1)} + E_j^{(2)}, \quad (8)$$

where $E_j^{(0)} = -JN$ is the flat band energy without interactions. The results are in good agreement with the numerical results, as shown in Fig. 2. The results also show the critical value of the Raman strength Ω for the flat band. The difference between the energy maximum E_{N+1} and minimum E_1 is

$$\Delta = -\frac{g^2 \Omega (N-1)}{8N(\Omega + 2J)(\Omega - 2J)}, \quad (9)$$

which is in good agreement with the numerical result shown in Fig. 3.

5. Conclusion

In summary, we show the energy spectrum of a tunable SOC BEC in a double-well potential through modulation of the Raman laser intensities. Such tunable spin-orbit coupling provides a powerful tool for exploring SOC superfluid physics in future experiments. For the single-particle spectrum, there is a flat band in the ground state, with the energy independent on the variation of the Raman strength. In this case, a system of N non-interacting bosons is characterized by an $(N+1)$ -fold degenerate state. Many-body interactions between atoms remove this high degeneracy, but the energy difference is very small. By using the perturbation theory with interaction as the perturbation, analytical results are obtained, which agree well with the numerical results. This results related to a huge degeneracy may lead to possible phases with non-trivial topological properties, and may have important applications in quantum information and quantum optics.

Acknowledgements

This work is supported by the National Fundamental Research Program of China (Contracts Nos. 2013CBA01502, 2011CB921503, and 2013CB834100) and the National Natural Science Foundation of China (Contracts Nos. 11374040, 11475027, 11274051 and 11125417).

References

- [1] Y.J. Lin, R.L. Compton, A.R. Perry, W.D. Phillips, J.V. Porto, I.B. Spielman, Phys. Rev. Lett. 102 (2009) 130401; Y.J. Lin, R.L. Compton, K.J. García, J.V. Porto, I.B. Spielman, Nature (London) 462 (2009) 628.
- [2] Y.J. Lin, K.J. García, I.B. Spielman, Nature (London) 471 (2011) 83.
- [3] Z. Fu, P. Wang, S. Chai, L. Huang, J. Zhang, Phys. Rev. A 84 (2011) 043609.
- [4] M. Aidelsburger, M. Atala, S. Nascimbène, S. Trotzky, Y.A. Chen, I. Bloch, Phys. Rev. Lett. 107 (2011) 255301.
- [5] J. Struck, C. Olschlager, R.L. Targat, P.S. Panahi, A. Eckardt, M. Lewenstein, P. Windpassinger, K. Sengstock, Science 333 (2011) 996.

- [6] J.Y. Zhang, S.C. Ji, Z. Chen, L. Zhang, Z.D. Du, B. Yan, G.S. Pan, B. Zhao, Y.J. Deng, H. Zhai, S. Chen, J.W. Pan, Phys. Rev. Lett. 109 (2012) 115301.
- [7] R.A. Williams, L.J. LeBlanc, K.J. García, M.C. Beeler, A.R. Perry, W.D. Phillips, I.B. Spielman, Science 335 (2012) 314.
- [8] Y.J. Lin, R.L. Compton, K.J. García, W.D. Phillips, J.V. Porto, I.B. Spielman, Nat. Phys. 7 (2011) 531.
- [9] P. Wang, Z.Q. Yu, Z. Fu, J. Miao, L. Huang, S. Chai, H. Zhai, J. Zhang, Phys. Rev. Lett. 109 (2012) 095301.
- [10] L.W. Cheuk, A.T. Sommer, Z. Hadzibabic, T. Yefsah, W.S. Bakr, M.W. Zwierlein, Phys. Rev. Lett. 109 (2012) 095302.
- [11] Y.P. Zhang, G. Chen, C.W. Zhang, Sci. Rep. 3 (2013) 1937.
- [12] M. Gong, S. Tewari, C. Zhang, Phys. Rev. Lett. 107 (2011) 195303.
- [13] H. Hu, L. Jiang, H. Pu, X.J. Liu, Phys. Rev. Lett. 107 (2011) 195304.
- [14] J.D. Koralek, C.P. Weber, J. Orenstein, B.A. Bernevig, S.C. Zhang, S. Mack, D.D. Awschalom, Nature (London) 458 (2009) 610.
- [15] D.W. Zhang, L.B. Fu, Z.D. Wang, S.L. Zhu, Phys. Rev. A 85 (2012) 043609.
- [16] Z.F. Yu, J.K. Xue, Phys. Rev. A 90 (2014) 033618.
- [17] J. Struck, J. Simonet, K. Sengstock, Phys. Rev. A 90 (2014) 031601(R).
- [18] M.A. Garcia-March, G. Mazarella, G.L. Dell'Anna, B. Juliá-Díaz, L. Salasnich, A. Polls, Phys. Rev. A 89 (2014) 063607.
- [19] R. Citro, A. Narddeo, arXiv:1405.5356.
- [20] C. Hamner, C.L. Qu, Y.P. Zhang, J.J. Chang, M. Gong, C.W. Zhang, P. Engels, Nat. Commun. 5 (2014) 4023.

UNCORRECTED PROOF